8th International Symposium on
Field Measurements in GeoMechanics
Berlin, Germany, September 12-16, 2011

Long-term geotechnical response of Venice coastal defences detected by Persistent Scatterer Interferometry

Luca Bincoletto,
Geological consultant, San Vito al Tagliamento, Italy
Paolo Simonini
IMAGE, University of Padova, Italy
Tazio Strozzi
Gamma Remote Sensing, Switzerland
Pietro Teatini
DMMMSA, University of Padova, Italy
Luigi Tosi
ISMAR, National Research Council, Venice, Italy

Abstract

With a surface area of about 550 km^2 the Venice Lagoon is the largest Italian wetland, open in the Upper Adriatic Sea to the highest tides of the Mediterranean Sea. The lagoon is connected to the sea through three inlets, which divide the narrow littoral strip separating the inner water body from the Adriatic. Several nearshore and offshore structures have been constructed over the decades to protect such a unique city and its coastal environment from sea storms and high waters, whose frequency and level are increasing due to relative sea level rise. Long jetties have been built at the inlets between the end of the 18th and beginning of the 19th centuries and then reinforced between 1994 and 1997. Since 2003, in the framework of the MOSE construction (i.e., the project of mobile barriers for the temporarily closure of the lagoon to the sea), the jetties have been extended, new breakwaters have been constructed in front of the inlets, and a small island has been realized within the Lido inlet to support the MOSE gates. An accurate quantification of the movements of these coastal defense structures due to long-term consolidation has been carried out by Persistent Scatterer Interferometry (PSI) using ENVISAT ASAR and TerraSAR-X images acquired from April 2003 to December 2009 and from March 2008 to January 2009, respectively. The displacements range between few mm/yr for the structures older than 10 years up to 50-70 mm/yr for those realized few years ago. The PSI measurements have been combined with the outcome of a detailed

Bincoletto, L., Simonini, P., Strozzi, T., Teatini, P. and Tosi, L. 2011. Long-term geotechnical response of Venice coastal defences detected by Persistent Scatterer Interferometry. In: 8th International Symposium on Field Measurements in GeoMechanics.
Berlin, Germany, September 12-16, 2011

geomechanical characterization of the lagoon subsoil down to -50 m depth below msl. The geotechnical dataset has been collected at a test site located on the northern littoral where an instrumented 20 m radius, 6.7 m high vertically-walled reinforced sand embankment was built at the end of 2002 and monitored till to 2007. The use of the derived stress-strain properties together with the actual lithostratigraphy below the structures, which is available from several piezocone profiles and boreholes, allow for the computation of secondary compression (consolidation) rates that match very well the PSI-derived movements. The results provide important information on the expected time-dependent settlement of these structures and prove the potentiality of PSI in controlling the geomechanical response of large coastal structures.

1 Introduction

The stability of coastal structures, such as breakwaters and jetties, is of considerable interest for engineering researchers, designers, and authorities responsible for their maintenance. Gradual deterioration can often pass unnoticed until weak areas give way to major damages. Potential movements induced by wave action, seepage, and construction weight are generally indicative of damaging. Moreover, the unexpected or underestimated reduction of the structure height with respect to the mean sea level is potentially threatening the construction integrity or reducing its effectiveness.

Therefore, short- and long-term monitoring programs are usually performed after the construction or restoration works to keep under control the settlement of these structures. Various measurement methods are employed in monitoring surveys. Commonly, levelling or GPS surveys are used to monitor the settlement of some selected benchmarks established at fixed intervals along the length of the structure (e.g., Rizos et al., 2010). Permanent GPS stations are used to measure three-dimensional coordinates of some chosen points (Del Grosso et al., 2003). More recently, terrestrial / low altitude aerial photogrammetry (e.g., Tsan-Wing and Kin-Wah, 2001) and laser scanning (e.g., Smith et al., 2010) methods have been used.

In this work we show the effectiveness of Persistent Scatterer Interferometry (PSI) to measure the long-term consolidation of coastal structures with high accuracy and resolution. With PSI, a number of satellite Synthetic Aperture Radar (SAR) scenes acquired over the same area at different times provide radar phase information that allows to detect and measure sub-centimeter ground movements. The technique is based on the

identification and exploitation of individual radar reflectors, or persistent scatterers (PS), that remain coherent over long time intervals so as to develop displacement time series (Ferretti et al., 2001; Werner et al., 2003). The resolution achieved by the identification of these PS in long temporal series of SAR images creates a data set consisting of many "radar benchmarks" where target displacement information can be accurately estimated due to favorable reflectivity conditions. PSI has been even more used over the last decade to measure land subsidence of large areas (e.g., Teatini et al., 2007; Mazzotti et al., 2009). More recently, the development of new very-high resolution X-band radar satellites, like the German TerraSAR-X and the Italian Cosmo-SkyMed missions, has increased the applicability of PSI to monitor the movements of single structures with millimetric precision and metric spatial resolution (e.g., Strozzi et al., 2009; Cuevas et al., 2011).

In this work we combine PSI with a large database of geomechanical and lithostratigraphic information to characterize the long-term geomechanical response of the coastal structures under construction or restoration at the inlets of the Venice Lagoon (Figure 1).

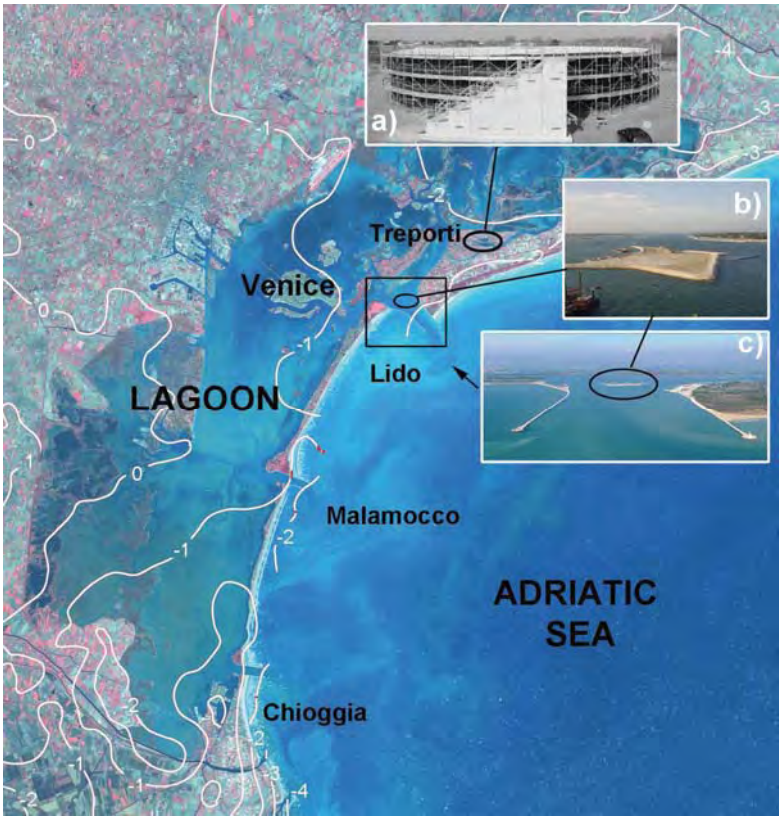

Figure 1: Satellite image of the Venice Lagoon showing the investigated sites: a) trial embankment at Treporti, b) artificial island and c) jetties at the Lido inlet. The white contour lines represent the average subsidence rates (mm/yr) over the period 2003-2009.

The sediments forming the upper 50 m of the Venetian lagoon basin consist of a very chaotic and heterogeneous assortment of interbedded normally consolidated or slightly overconsolidated silts, medium-fine silty sands and silty clays. As a consequence high variability of the displacements measured by PSI is observed also in relatively small areas (Tosi et al., 2010).

These soils are intrinsically hard to be characterised in the laboratory because of the spatial heterogeneity and the difficulty to sample them (Cola and Simonini, 2002). Thus, an instrumented trial embankment was build next to the Lido inlet (Simonini, 2004) in order to investigate the lagoon subsoil response to loading and to assess the relevant geotechnical design parameters accounting for the macrostructural feature of the deposits. The long-term settlement due to secondary compression of the Venice coastal defences calculated using these data are shown to match very well the vertical movements of the structures measured by PSI from 2003 to 2009 using ENVISAT and TerraSAR-X images.

2 General setting of the study area

2.1 Geological setting

The Venice area is part of the Po plain, a foreland region located between the NE-verging northern Apenninic and the SSE-verging eastern South-Alpine chains. The first 50-70 m subsoil thick, i.e. the deposits object of this study, is composed of late Pleistocene and Holocene sedimentations. The stratigraphic setting of the Venice area was carried out by multidisciplinary analysis from sediment cores and very high resolution seismic (VHRS) surveys (e.g., Canali et al., 2007; Zecchin et al., 2008; Tosi et al., 2009; Rizzetto et al., 2010) (Figure 2). The boundary with the overlying Holocene units is often characterized by the presence of a paleosoil, locally named caranto, which developed in conditions of prolonged subaerial exposure and sedimentation starving (e.g., Brambati et al., 2003; Bonardi et al., 2006 and references within). The caranto is mainly composed of very stiff clayey silts or silty clays. The Holocene architecture shows a rather complex sequence due to changes of the relative sea level and sediment supply and, over the last millennium, as the result of human-induced river diversions and engineering interventions (Madricardo et al., 2007; Donda et al., 2008; Tosi et al., 2009). The Holocene sequence is composed of fluvial, back barrier, deltaic and shoreface deposits forming a transgressive-regressive cycle.

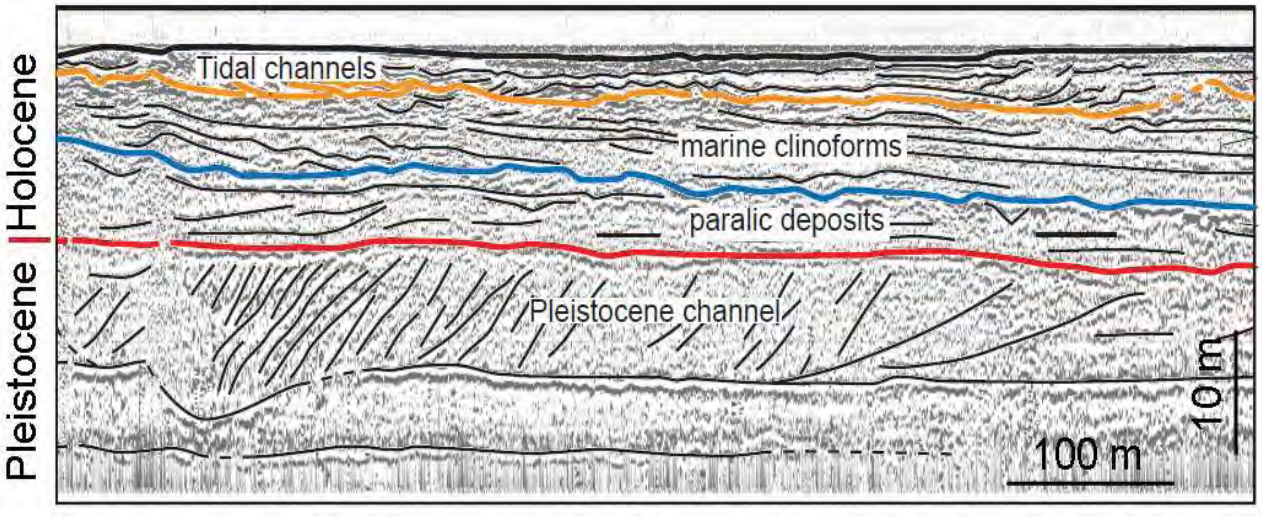

Figure 2: Interpreted VHRS profile showing the complexity-heterogeneity of the Venice lagoon subsoil (modified from Zecchin et al., 2009 and Rizzetto et al., 2010).

2.2 Regional land subsidence

Land subsidence monitoring in the Venice coastland has been significantly improved over the last few years by space borne earth observation techniques based on SAR interferometry as Differential InSAR (DInSAR) and PSI (e.g., Tosi et al., 2002; Wegmüller et al., 2004; Teatini et al., 2005; Teatini et al., 2007; Strozzi et al., 2009). High reliable land subsidence data have been detected for thousands of PS located on the lagoon margins, along the littorals, in major and small islands, and on single anthropogenic structures scattered within the lagoon.

High resolution maps of the ground vertical movements both at “regional” (100×100 km^2) and “local” (few km^2) scales have been obtained (Teatini et al., 2005; Teatini et al., 2010; Tosi et al., 2010). The general picture of the land displacements at the Venice coastland shows a significant spatial variability with velocities ranging from a slight uplift (1–2 mm/yr) to a significant subsidence of more than 10 mm/yr (Figure 1). The subsidence depends on both local geologic conditions and anthropogenic activities. Tectonics, differential consolidation of the Pleistocene and Holocene deposits, and human activities, such as groundwater withdrawals, land reclamation of marshes and swamp areas, and farmland conversion into urban areas, superimpose to produce the observed displacements (Tosi et al., 2009). In particular, the regional displacement rates in the coastal area of interest range from -1 to -2 mm/yr.

3 Ground displacements by PSI

In DInSAR, a pair of SAR images acquired from slightly different orbit configurations and at different times is combined to exploit the phase difference of the signals, commonly termed "interferogram" (Bamler and Hartl, 1998; Rosen et al., 2000). The interferometric phase Φ is sensitive to both the coherent displacement along the look vector occurring between the acquisitions of the interferometric image pair Φ_{DISP} and the residual topographic signal due to inaccurate removal of the topographic phase contribution caused by the different orbital positions Φ_{TOPO}, with changes in atmospheric conditions Φ_{ATMO} (temperature, moisture content, pressure), and phase noise Φ_{NOISE} introducing the main error sources:

$$\Phi = \Phi_{DISP} + \Phi_{TOPO} + \Phi_{ATMO} + \Phi_{NOISE} \quad (1)$$

Because interferometric displacement analyses use Eq. (1) to estimate the displacement phase Φ_{DISP}, which is then converted to range displacement in the direction of the sensor's line-of-sight (LOS), the last three terms must be considered contributions to the measurement error and must be eliminated or at least moderate. The importance of Φ_{TOPO} depends on the accuracy of the available topographic information, e.g. the DEM, and the interferometric baseline, which is a function of the orbital geometries. Lowlying coastal areas often are characterized by relatively flat topography and the resulting phase error due to uncompensated topography is often negligible. The atmospheric phase Φ_{ATMO} can introduce errors corresponding to surface displacements of up to a few centimetres, particularly in hot and humid climates. However, atmospheric signal contributions generally are not repeated in independent interferograms. Where multiple observations are available, gross misinterpretations of atmospheric signals can be avoided. Finally, Φ_{NOISE} primarily depends on the signal-to-noise ratio limiting factor, which depends on the orbital distance between the two acquisition tracks projected into the LOS (spatial decorrelation) and on the amount of temporal change occurring between the two acquisitions (temporal decorrelation).

With DInSAR, the measurement of the radar phase change is generally made on a pixel-resolution basis, although the actual resolution is usually lower, as the filtering procedures reduce the noise level at the expense of the spatial resolution. Differently, the persistent scatterer interferometry involves the processing of several, typically more than 30, interferograms to identify a network of persistent, temporally stable, highly reflective ground features that are smaller than the resolution pixel cell and that remain coherent

over long time intervals. Because the dimension of these targets is much smaller than the resolution cell, almost no spatial decorrelation occurs, permitting interpretation of the interferometric phase of pairs with long baselines. Temporal decorrelation is avoided or strongly reduced too, as the interferometric investigation is focussed on temporally stable targets in the image (Ferretti et al., 2001). The phase history of each PS is extracted to supply its average annual displacement rate and the displacement history, up to the length of a SAR data archive, thus providing a refined “virtual” network of levelling benchmarks monitored with a 10 to 35 day frequency depending on the satellite revisit time.

From early 2000’s, PSI has been widely applied in the northern Adriatic coastland from the Po River to the south to the Tagliamento River northward, and particularly in the Venice Lagoon, with the main goal of monitoring land subsidence which is still one of the major environmental processes threatening this lowlying coastal area (Teatini et al., 2007, 2010; Strozzi et al., 2009; Tosi et al., 2009). Various satellite images have been processed by IPTA (Werner et al., 2003; Wegmüller et al., 2004), one of the PSI processing-chain available at present.

In this work we used 64 scenes ENVISAT (35 days repeat cycle, ~25 m pixel dimension) acquired from 2003 to 2009 and a total of 30 TerraSAR-X stripmap images (11 days repeat cycle, ~3 m pixel dimension) acquired in 2008-2009 to measure the long-term geotechnical response of coastal defences in the northern part of the Venice lagoon.

4 Test sites

4.1 Trial embankment at Treporti

A comprehensive investigation was carried out at Treporti, 5 km North of the Lido inlet, where a field scale experiment was performed to characterize the geomechanical properties of the lagoon subsoil (Simonini, 2004; Simonini et al., 2006; Jamiolkowski et al., 2009).

A 6.5 m high, 40 m diameter, geogrid-reinforced vertical-walled cylindrical test bank was constructed from September 2002 to March 2003, and removed in 2008. The picture of the cylindrical embankment and a plan view showing the monitoring instrumentation position are illustrated in Figure 1 and Figure 3, respectively. The subsoil was heavily instrumented allowing to measure settlement, horizontal displacement and the pore pressure at different location below the embankment during its whole life. Four sliding deformeters were installed at 1 m depth intervals to measure the vertical displacements with an accuracy of

0.03mm/m. These devices permitted to compute the vertical strain (ε_z) and its evolution achieving a deeper in-situ insight into the primary and secondary compression phenomena.

Figure 3 shows the construction history and the settlement of the ground surface measured below the centre of the trial embankment, where the stress and deformation field approaches the 1-D compression condition. Note that the displacements measured by three methods, namely levelling, GPS, and sliding deformeter, practically coincide during the entire 6-year monitoring period. In addition, the total vertical displacement provided by the sliding deformeters established at a 15-m radius is comparable with those obtained by PSI on a couple of reflectors located at the embankment site (Figure 4b). The PSI application on the Treporti area has allowed to detect the present local subsidence and the occurrence of higher consolidation rates of local structures such as the trial embankment and other buildings recently constructed or restored.

A through characterization of the subsoil was carried out by in situ tests and laboratory experiments on undisturbed samples. The results show that the soil profile below the test site is described as follows (Figure 4a):

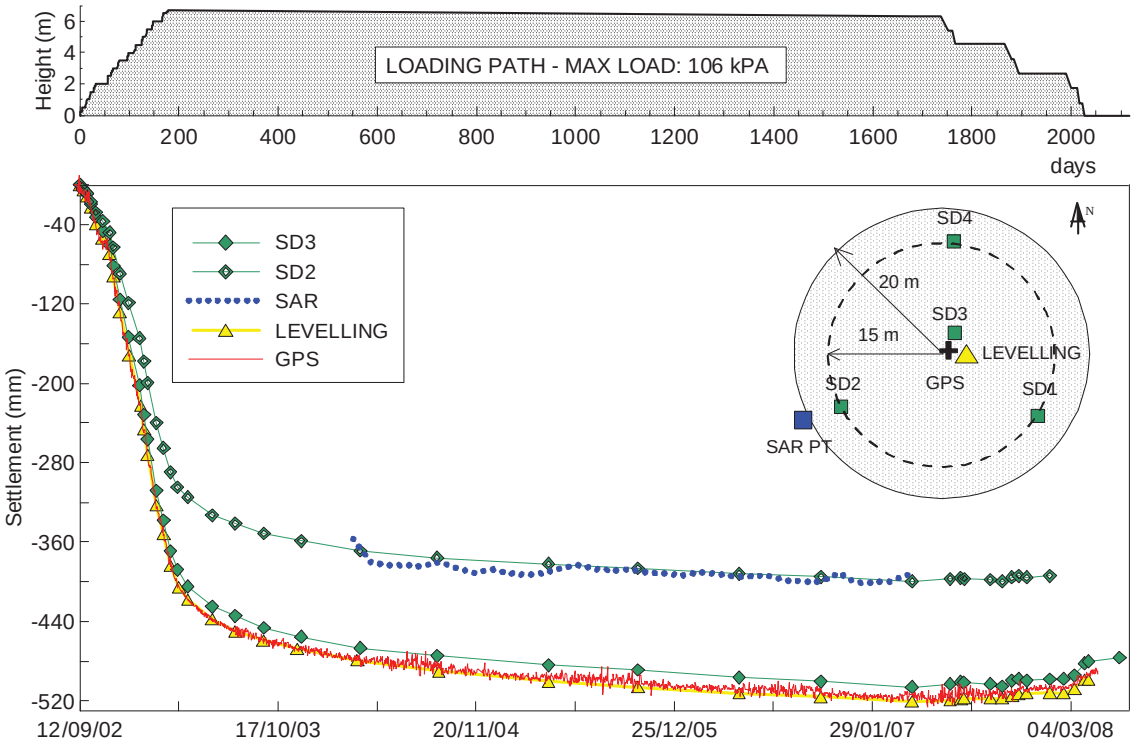

Figure 3 : Settlement vs. time measured with levelling, GPS, sliding deformeters, and PSI at the center and the edge of the Treporti trial embankment. The instrument locations with respect to the embankment are shown on the top-right inset.

- 1 to 3 m: soft silty clay (layer A),
- 3 to 8 m: medium to fine silty sand (layer B),
- 8 to 20 m: clayey and sandy silt with sand laminations at depth between 15 and 18 m (layer C),
- 20 to 22 m: medium-fine silty sand (layer D),
- 22 to 45 m: alternating layers of clayey and sandy silt (layer E),
- 45 to 55 m: medium-fine silty sand (layer F),

and can be summarized by the following lithological percentages: sands and slightly silty sands 22%, sandy silts and silts 32%, inorganic silty clays 37%, and organic clays plus peat 9%.

Primary consolidation developed almost entirely during the embankment construction. This is supported by the negligible pore overpressure measured by the piezometers after the end of the built up phase. The sliding deformeter located below the embankment centre provided a clear distribution of the vertical displacements and of ε_z versus depth. Excluding the upper layer A, the differential displacements are mostly concentrated in the silty formation C. The thick continuous line marks the bank completion. ε_z does not exceed 4% in all the layers B, C, D and E and vanishes at approximately 40 m depth. Typical ε_z vs. time curves is characterized by the typical *S-type* shape in a semilog plane with the first part representing the primary compression and the final portion corresponding to long term behaviour occurring after bank construction. This latter is due to secondary compression (creep), i.e. the decrease of soil porosity driven by the viscous compression of solid skeleton at constant load, and can be reasonably fitted by a straight line whose slope is assumed to be the site secondary compression coefficient:

$$C_{\alpha\varepsilon} = -\frac{\Delta\varepsilon_z}{\Delta \log t}$$

The values of $C_{\alpha\varepsilon}$ have been inferred from the sliding deformeter readings and laboratory measurements (Figure 5). Typical values of secondary compression coefficient $C_{\alpha\varepsilon}$ for the typical classes of Venice lagoon subsoil may be roughly assumed as follows:

- sands and silty sands: $1.0\text{-}1.5\times10^{-3}$;
- clayey silts and silty clays with organic laminations: $2.5\text{-}4.0\times10^{-3}$.

The secondary settlement s_{sec} of a structure (i.e. embankment, jetty, breakwater in the present study) stressing a normally-consolidated heterogeneous soil can be computed at time t by the following equation:

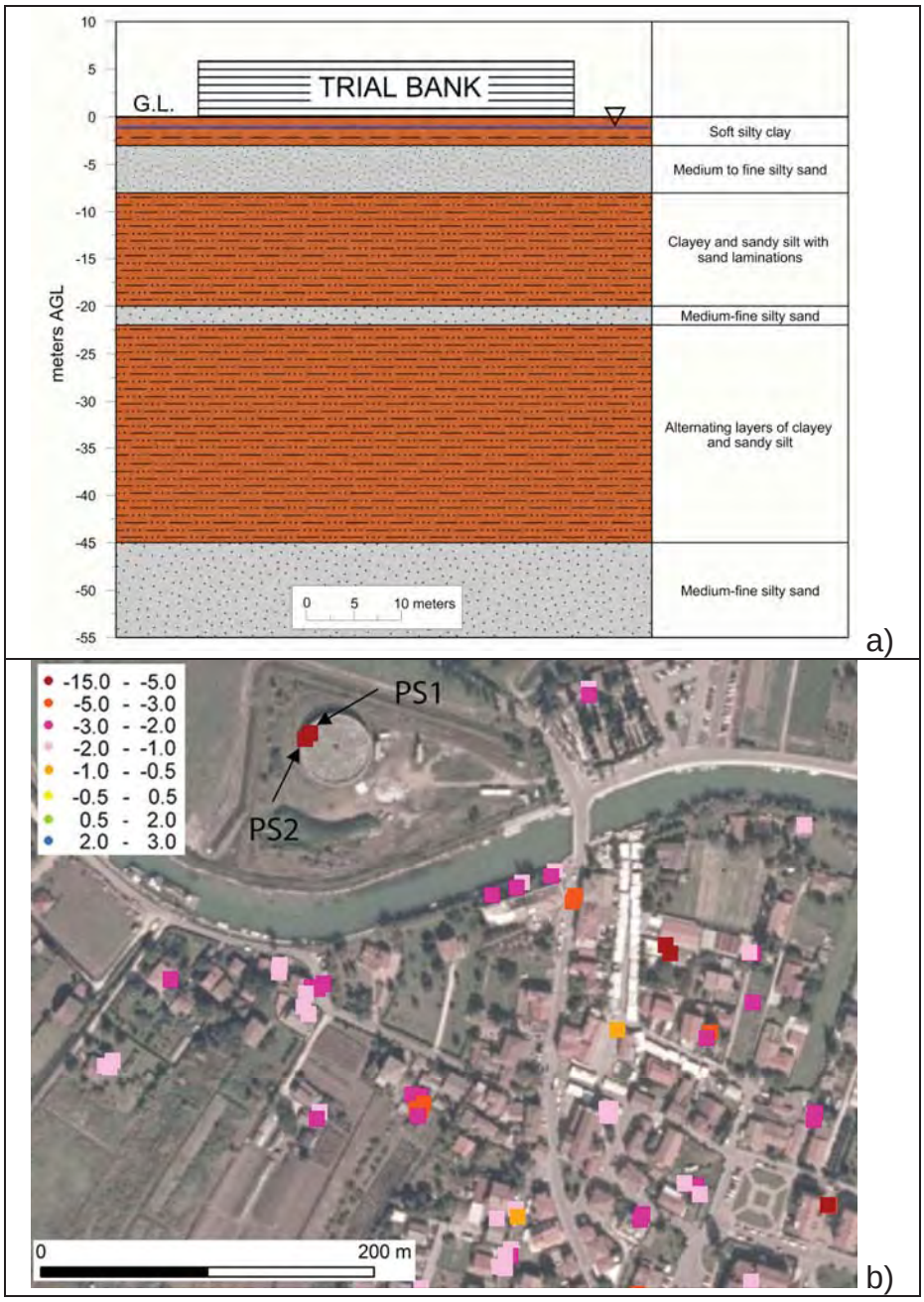

Figure 4: Treporti area. a) Sketch of the embankment and the stratigraphic sequence below the structure. b) Average displacement rate (mm/yr) obtained from 2003 to 2009 obtained by IPTA on ENVISAT images. Negative values indicate settlement. PS1 and PS2 are two reflectors placed on the embankment.

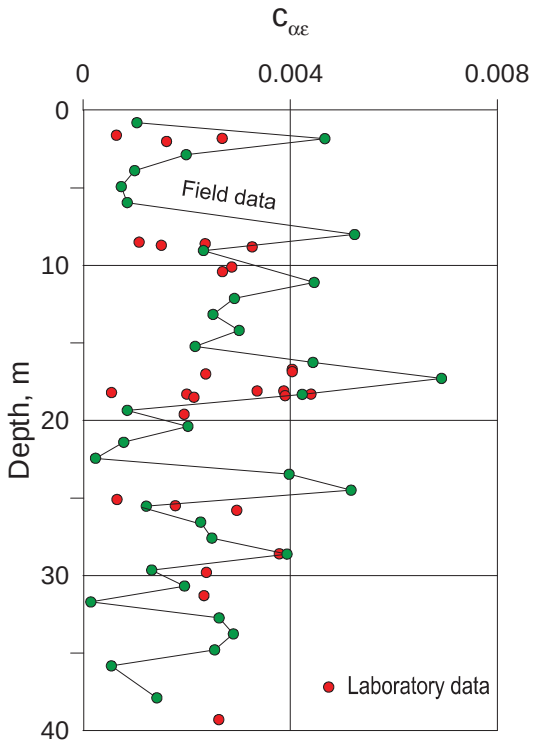

Figure 5: Secondary compression coefficient vs. depth obtained by field and laboratory measurements at the Treporti site.

$$s_{sec} = \sum_{i=1}^{n} H_i \cdot C_{\alpha\varepsilon i} \cdot \log\left(\frac{t}{t_{ref}}\right) \tag{2}$$

where n is the number of layers forming the subsoil, H_i and $C_{\alpha\varepsilon i}$ are the thickness and secondary compression coefficient of each layer, respectively, and t_{ref} is the reference time for calculating secondary settlement, i.e. the time at which primary consolidation ended.

4.2 Coastal structures at the Lido inlet

Until 1800 the Lido inlet was shallow, less than 2 m deep, and wide, larger than 2000 m, and composed of three secondary inlets. Sedimentary process and dynamics of the bottom morphology caused the shoaling of the navigation channel. In order to stabilize the inlet morphology, two jetties were built between 1890 and 1910. Starting from the middle 1990's, in the framework of the MOSE works, the jetties were strongly reinforced. Moreover, an artificial island was constructed at the centre of the Lido inlet. The construction of the island, which is composed by a sandy nucleus bounded by a stone breakwater, started in 2005. The built up of the 8 m high and 5-27 m large embankment mostly finished in 2007.

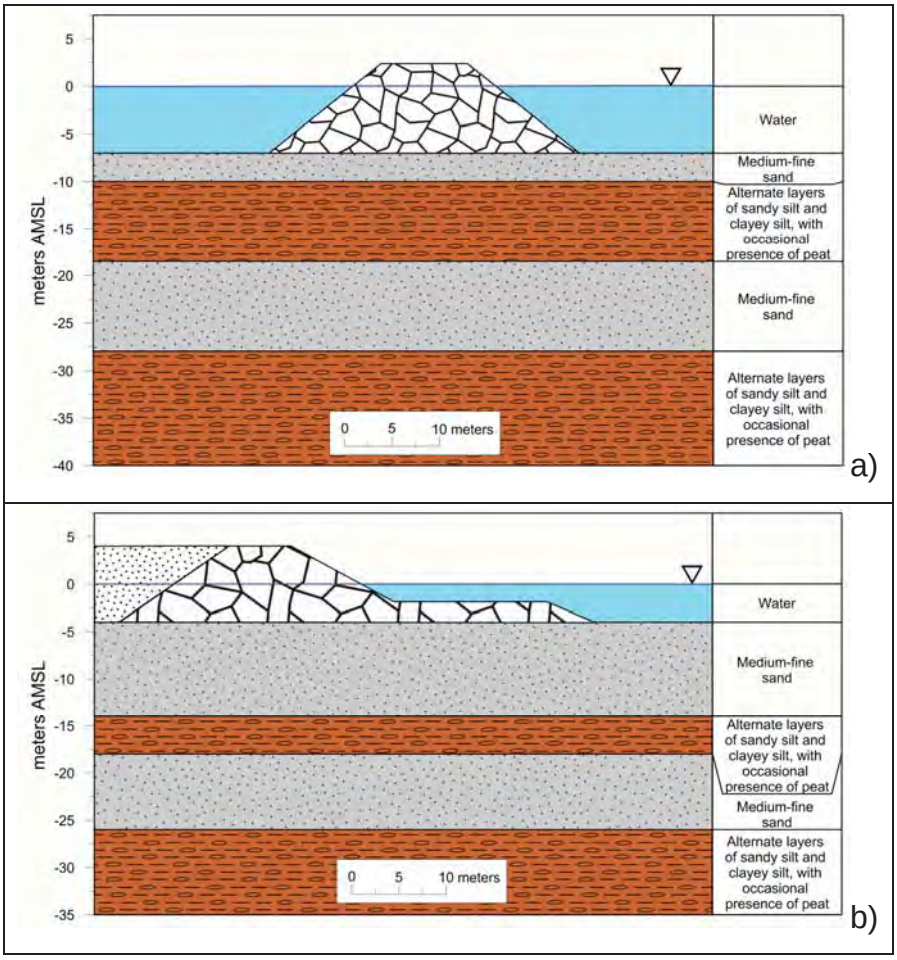

Figure 6: Sketch of a) the southern jetty constructed at the Lido Inlet with the stratigraphic sequences below the structures and b) the embankment confining the artificial island.

A schematic representation of the structures and subsoil of the southern jetty and the artificial island is shown in Figure 6. The section of the jetty is located at a sea depth of about 7 m corresponding to a central part of the structure not affected by the recent works carried out for the MOSE construction (Figure 7). The stratigraphic characterizations were provided by several boreholes and piezocone penetration tests carried out to plan the jetties reinforcing and the island construction. Note the subsoil variability between the two sites due to the complex evolution history of the area.

In order to detect the long- term displacements related to the secondary settlement of the costal structures, ENVISAT and TerraSAR-X images have been used. The number of PS detected by TerraSAR-X is much larger than that detected by ENVISAT due to the higher spatial resolution of the latter and the lost of signal coherence during the longer ENVISAT acquisition interval caused by morphological changes of the reflectors. Note the lack of PS

from the ENVISAT analysis in the portion of the two jetties closer to the littoral (Figure 7a) whereas hundreds of reflectors showing sinking rates higher than 20 mm/yr have been detected by TerraSAR-X in the late shorter period. These parts of the jetties were strongly modified from 2005 to 2007 and the radar reflectors destroyed.

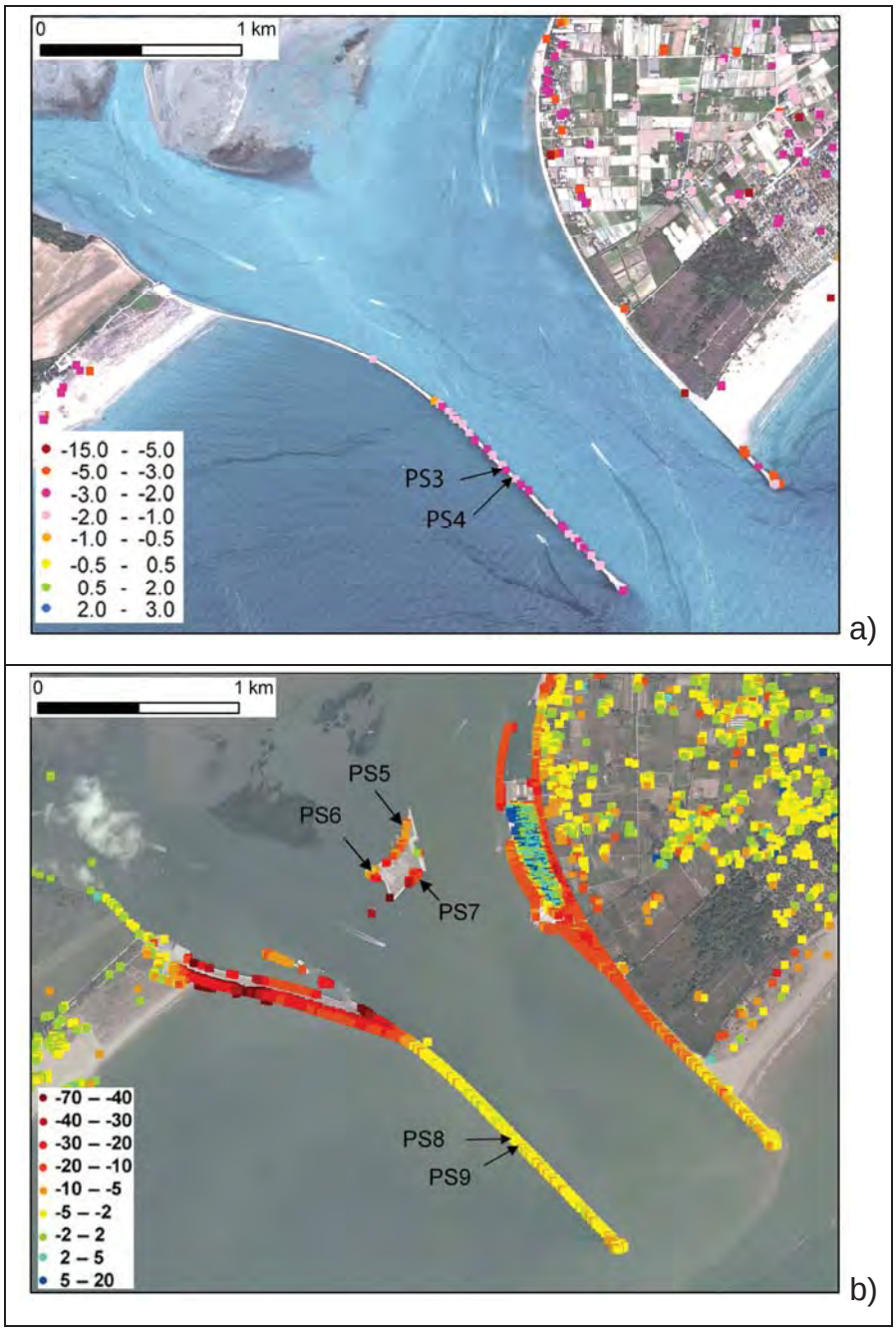

Figure 7: IPTA results at the Lido inlet (mm/yr). a) 2003-2009 average displacement rates from ENVISAT and b) 2008-2009 displacement rates from TerraSAR-X images. The backgrounds are a QUICKBIRD and an aerophotograph acquired in 2003 and 2008, respectively. Negative values indicate settlement, positive mean uplift. The displacement histories of the reflectors highlighted in the two maps are provided in Figure 8.

Sinking rates on the order of 1-2 mm/yr detected along the littoral strips represent the local present natural subsidence in the Lido area (see also Figure 1). Higher values are generally induced by groundwater pumping and engineering interventions carrying out in the framework of the MOSE works. The consolidation rates of the breakwater containing the new artificial island are generally greater than 5 mm/yr.

5 Integrated analysis

Equation (2) has been applied to calculate the long-term settlement of the structures at the Lido inlet due to secondary consolidation. The geotechnical characterization of the various litho-types achieved by the Treporti experiment has been used. Table 1 summarizes the data used for the computation. In agreement with the end of the restoration/construction activities, the reference time t_{ref} are set to January 1996 and 2007 for the jetty and the artificial island, respectively. As suggested by the measurements at the Treporti test site, the subsoil thickness affected by secondary compression correspond to the structure dimension at the sea bottom.

Lido southern jetty				
Top depth (m below seabed)	**Bottom depth (m below seabed)**	**Thickness (m)**	**Lithology**	**Cα**
0	3	3	Medium-fine sand	0.001
3	11.5	8.5	Alternate layers of sandy silt and clayey silt, with occasional presence of peat	0.004
11.5	21	9.5	Medium-fine sand	0.001
21	33	12	Alternate layers of sandy silt and clayey silt, with occasional presence of peat	0.004
Lido artificial island				
Top depth (m below seabed)	**Bottom depth (m below seabed)**	**Thickness (m)**	**Lithology**	**Cα**
0	10	10	Medium-fine sand	0.001
10	14	4	Alternate layers of sandy silt and clayey silt, with occasional presence of peat	0.004
14	21	7	Medium-fine sand	0.001
21	27	6	Alternate layers of sandy silt and clayey silt, with occasional presence of peat	0.004

Table 1: Geotechnical and lithostratigraphic characterization of the subsoil for the two structures addressed by the present study and used to apply equation (2).

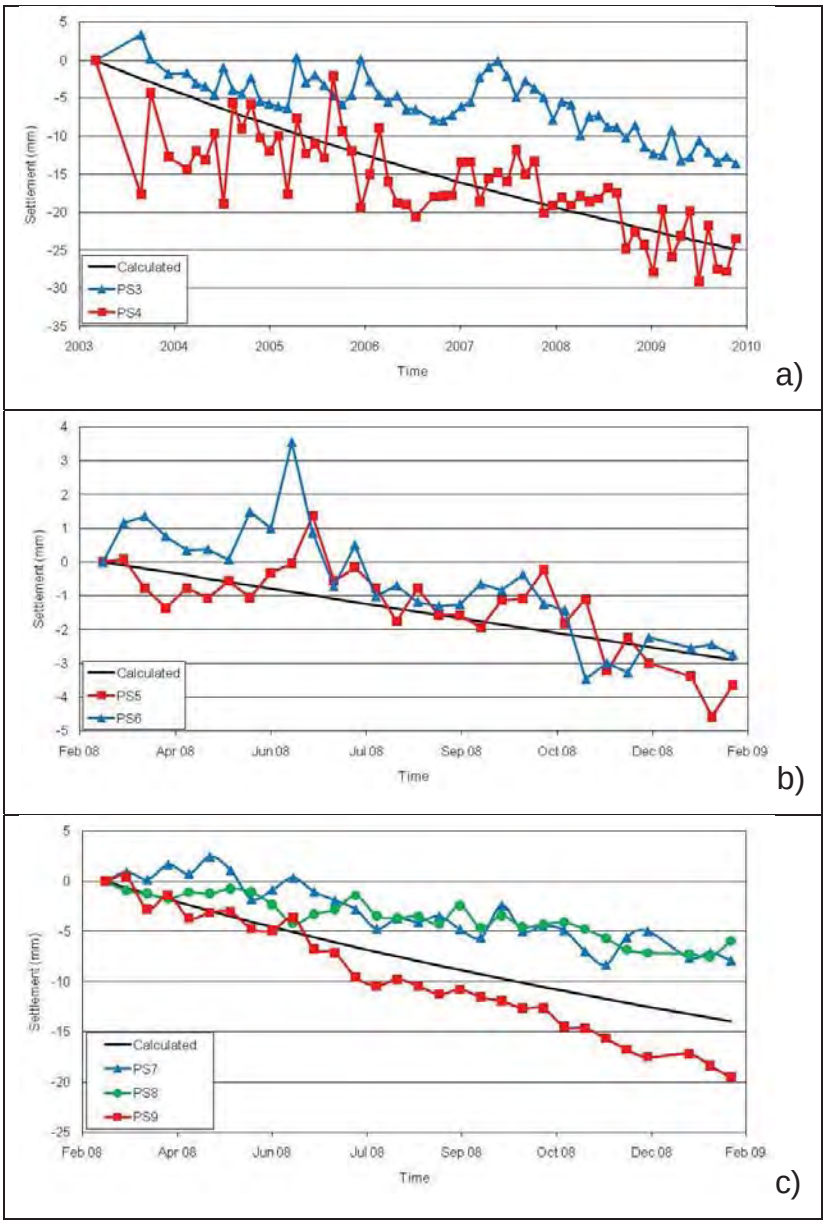

Figure 8: Comparison between the secondary settlement calculated using equation (2) and the measurements provided by IPTA on a few PS. a) and b) central part of the southern jetty over the 2003-2009 and 2008-2009 periods, respectively; c) embankment of the artificial island from 2008 to 2009. The PS locations are shown in Figure 7.

The results of the calculation are shown in Figure 8. Figure 8 also provides the displacement measured by IPTA on a few PS located in correspondence of the portion of the structures where the computation was performed. Note the general good agreement between the records and the simulated movements. A more detailed investigation shows that:

- the calculated trend for the jetty fits satisfactory the available measurements provided from TerraSAR-X (Figure 8b) and ENVISAT (Figure 8a) if a simple translation of the PS3 origin is introduced;
- the outcome of the calculation falls within the range of the IPTA measurements for the island. A certain difference in the displacement obtained by IPTA is expected as the seaward portion of the breakwater seems reinforced and is directly affected by the waves entering the inlet.

6 Conclusions

We have shown that PSI is a powerful technique to measure long-term displacements of large structures such as coastal constructions. PSI provides an impressive number of monitoring points with an almost metric spatial resolution and a millimetric precision over time intervals from one to several years, which cannot be obtained by other monitoring methods. The large dataset allows capturing the high variability of the displacement rates along a single structure that are caused to the subsoil heterogeneity, the construction history and dimensions.

In the Venice area, where a large lithostratigraphic and geotechnical database is available, the movement of the structures at the lagoon inlets detected by PSI from 2003 to 2009 using ENVISAT and TerraSAR-X images match satisfactory the secondary consolidation computed using the outcome of an in-situ field-scale test carried out at Treporti.

The results are very interesting from different points of view:

- an accurate geomechanical characterization of the various lithotypes composing the subsoil of the Venice lagoon allows for a reliable quantification of long-term settlement of structures located in different parts of the coastal area once the stratigraphy is known;
- with the new very-high resolution X band satellites only one year of acquisition suffices to detect a reliable consolidation trend of large coastal structures.

Finally, from the above considerations we can conclude that PSI provides an accurate monitoring of structure displacements over very large areas and several years. This method represents a unique and relatively economical tool for a careful back-analysis of on-site soil mechanical response and allows for the validation of the consolidation prediction methods in heterogeneous subsoil, otherwise not easily affordable with the traditional measurement techniques.

Acknowledgments

TerraSAR-X data courtesy COA0612, ©DLR. ENVISAT ASAR data ©ESA. ENVISAT data have been elaborated within the INLET Project supported by Magistrato alle Acque (Venice Water Authority) through its concessionary Consorzio Venezia Nuova. Relevant geotechnical and engineering information courtesy of Venice Water Authority and Consorzio Venezia Nuova.

References

R. Bamler; P. Hartl; Synthetic aperture radar interferometry, *Inverse Problem, 14, R1–R54, 1998*

M. Bonardi; L. Tosi; F. Rizzetto; G. Brancolini; L. Baradello; Effects of Climate Changes on the Upper Pleistocene and Holocene Sediment of the Venice Lagoon, Italy, *Journal of Coastal Research, SI39, 279-284, 2006*

A. Brambati; L. Carbognin; T. Quaia; P. Teatini; L. Tosi; The Lagoon of Venice: geological setting, evolution and land subsidence, *Episodes, 26(3), 264-268, 2003*

G. Canali; L. Capraro; S. Donnici; F. Rizzetto; R. Serandrei Barbero; L. Tosi; Vegetational and environmental changes in the eastern Venetian coastal plain (Northern Italy) over the past 80,000 years*, Palaeogeography, Palaeoclimatology, Palaeoecology, 253, 300-316, 2007*

S. Cola; P. Simonini; Mechanical behaviour of silty soils of the Venice lagoon as a function of their grading properties, *Canadian Geotechnical Journal, 39(4), 879-893, 2002*

M. Cuevas; M. Crosetto; O. Monserrat; Monitoring urban deformation phenomena using satellite images, *in 9th Int. Geomatic Week, Barcelona, Spain, 15-17 March, 2011*

A. Del Grosso; F. Lanata; D. Inaudi; D. Posenato; A. Pieracci; Breakwater deformation monitoring by automatic and remote GPS system, in Wu & Abe (eds.), *Structural Health Monitoring and Intelligent Infrastructure, Proc. Int. Conf. SHMII-1, Taylor & Francis Group, November 2003 in Tokyo, vol. 2, p. 369-376, 2003*

F. Donda; G. Brancolini; L. Tosi; V. Kovacevic; L. Baradello; M. Gacic; F. Rizzetto; The ebb-tidal delta of the Venice Lagoon, Italy, *The Holocene, 18(2), 267-278, 2008*

A. Ferretti; C. Prati; F. Rocca; Permanent scatterers in SAR interferometry, *IEEE Transaction on Geoscience and Remote Sensing, 39(1), 8−20, 2001*

M. Jamiolkowski; G. Ricceri; P. Simonini; Safeguarding Venice from high tides: site characterization & geotechnical problems, *XVII ICSMGE, October 5-9, 2009 in Alexandria, Egypt, 2009*

F. Madricardo; S. Donnici; S. Buogo; P. Calicchia; A. Lezziero; F. De Carli; E. Boccardi; Palaeoenvironment reconstruction in the Lagoon of Venice through wide-area acoustic surveys and core sampling, *Estuarine, Coastal and Shelf Science, 75, 205-213, 2007*

S. Mazzotti; A. Lambert; M. Van der Kooij; A. Mainville; Impact of anthropogenic subsidence on relative sea-level rise in the Fraser River delta, *Geology, 37, 771–774, 2009*

C. Rizos; J. van Cranenbroeck; V. Lui; Advances in GNSS-RTK for structural deformation monitoring in regions of high ionospheric activity, XXIV *FIG Congress 2010, April 11-16, 2010 in Sydney, 2010*

F. Rizzetto; L. Tosi; M. Zecchin; G. Brancolini; Modern geological mapping and subsurface lithostratigraphic setting of the Venice Lagoon (Italy), *Rendiconti Lincei-Scienze Fisiche e Naturali, 21, Suppl. 1, 239-252, 2010*

P. Rosen; S. Hensley; I. Joughin; F. Li; S. Madsen; E. Rodriguez; R. Goldstein; Synthetic Aperture Radar interferometry, *Proc. IEEE, 88(3), 333−382, 2000*

P. Simonini; Characterization of the Venice lagoon silts from in-situ tests and the performance of a test embankment, *Proc. ISC'02, Geotechnical and Geophysical Site Characterization, 1, p. 187-207, Rotterdam, Millpress, 2004*

P. Simonini; G. Ricceri; S. Cola; Geotechnical characterization and properties of the Venice lagoon heterogeneous silts*, Invited lecture, 2nd Int. Workshop on Characterization and Engineering Properties of Natural Soils, Singapore, 4, p. 2289-2328, London, Taylor & Francis, 2006*

T. D. Smit; J. Podoski; J. Goo; Monitoring of a Core-Loc ® breakwater in Lanai, Hawaii, *23rd Annual National Conference on Beach Preservation Technology, February 3-5, 2010 in Indialantic (Florida), 2010*

T. Strozzi; P. Teatini; L. Tosi; TerraSAR-X reveals the impact of the mobile barrier works on Venice coastland stability, *Remote Sensing of the Environment, 113(12), 2682-2688, 2009*

P. Teatini; L. Tosi; T. Strozzi; L. Carbognin; U. Wegmüller; F. Rizzetto; Mapping regional land displacements in the Venice coastland by an integrated monitoring system, *Remote Sensing of the Environment, 98(4), 403−413, 2005*

P. Teatini; T. Strozzi; L. Tosi; U. Wegmüller; C. Werner; L. Carbognin; Assessing short- and long-time displacements in the Venice coastland by synthetic aperture radar interferometric point target analysis, *Journal of Geophysical Research, 112, F01012, doi:10.1029/2006JF000656, 2007*

P. Teatini; L. Tosi; T. Strozzi; L. Carbognin; G. Cecconi; R. Rosselli; S. Libardo; Resolving land subsidence within the Venice Lagoon by persistent scatterer SAR interferometry, *Physics and Chemistry of the Earth, doi:10.1016/j.pce.2010.01.002, 2010*

L. Tosi; L. Carbognin; P. Teatini; T. Strozzi; U. Wegmüller; Evidence of the present relative land stability of Venice, Italy, from land, sea, and space observations, *Geophysical Research Letters, 29(12), 1562, 2002*

L. Tosi; F. Rizzetto; M. Zecchin; G. Brancolini; L. Baradello; Morphostratigraphic framework of the Venice Lagoon (Italy) by very shallow water VHRS surveys: Evidence of radical changes triggered by human-induced river diversion, *Geophysical Research Letters, 36, L09406, 2009*

L. Tosi; P. Teatini; L. Carbognin; Brancolini; Using high resolution data to reveal depth-dependent mechanisms that drive land subsidence: The Venice coast, Italy, *Tectonophysics, 474, 271−284, 2009*

L. Tosi; P. Teatini; T. Strozzi; L. Carbognin; G. Brancolini; F. Rizzetto; Ground surface dynamics in the northern Adriatic coastland over the last two decades, *Rendiconti Lincei-Scienze Fisiche e Naturali, 21, Suppl. 1, 115-129, 2010*

N. G. Tsan-wing; L. Kin-wah; Application of photogrammetry in monitoring of marine rubble structures, *The 10th FIG International Symposium on Deformation Measurements, March 19-22, 2001 in Orange (California), p. 42-49, 2001*

M. Zecchin; L. Baradello; G. Brancolini; F. Donda; F. Rizzetto; L. Tosi; Sequence stratigraphy based on high resolution seismic profiles in the late Pleistocene and Holocene deposits of the Venice area, *Marine Geology, 253, 185–198, 2008*

M. Zecchin; G. Brancolini; L. Tosi; F. Rizzetto; M. Caffau; L. Baradello; Anatomy of the Holocene succession of the southern Venice Lagoon revealed by very high resolution seismic data, *Continental Shelf Research, 29(10), 1343-1359, 2009*

U. Wegmüller; C. Werner; T. Strozzi; A. Wiesmann; Multitemporal interferometric point target analysis. In: P. Smits, L. Bruzzone (Eds.), *Analysis of Multi-temporal Remote Sensing Images, Hoboken N. J., World Sci., Ser. Remote Sens., 3,136−144, 2004*

C. Werner; U. Wegmüller; T. Strozzi; A. Wiesmann; Interferometric Point Target Analysis for deformation mapping. Paper presented at IGARSS 2003, *Inst. of Electr. and Electron. Eng., New York, 2003*

Authors

Dr.-Geol. Luca Bincoletto luca.bincoletto@gmail.com
Geological consultant
Via San Carlo 44, 33078 San Vito al Tagliamento, Italy

Prof.-Ing. Paolo Simonini paolo.simonini@unipd.it
Dept. of Hydraulic, Maritime, Environmental, and Geotechnical Engineering
University of Padova
Via Ognissanti 39, 35129 Padova, Italy www.image.unipd.it

Dr. Tazio Strozzi strozzi@gamma-rs.ch
GAMMA Remote Sensing AG
Worbstrasse 225, CH-3073 Gümligen, Switzerland www.gamma-rs.ch

Dr.-Ing. Pietro Teatini teatini@dmsa.unipd.it
Dept. of Mathematical Methods and Model for Scientific Applications
University of Padova
Via Trieste 63, 35121 Padova, Italy www.dmsa.unipd.it

Dr.-Geol. Luigi Tosi luigi.tosi@ismar.cnr.it
Institute of Marine Sciences
National Research Council
Arsenale - Tesa 104, Castello 2737/F, 30122 Venezia, Italy www.ismar.cnr.it

Bincoletto, L., Simonini, P., Strozzi, T., Teatini, P. and Tosi, L. 2011. Long-term geotechnical response of Venice coastal defences detected by Persistent Scatterer Interferometry. In: 8th International Symposium on Field Measurements in GeoMechanics. Berlin, Germany, September 12-16, 2011